Photoacoustic evaluation of the thermal diffusivity of coconut shell

2002 J. Phys.: Condens. Matter 14 4509

(http://iopscience.iop.org/0953-8984/14/17/321)

INSTITUTE OF PHYSICS PUBLISHING JOURNAL OF PHYSICS: CONDENSED MATTER

J. Phys.: Condens. Matter **14** (2002) 4509–4513 PII: S0953-8984(02)34494-1

Photoacoustic evaluation of the thermal diffusivity of coconut shell

Nibu A George[1,3] **and R Vinayakrishnan**[2]

[1] Thermal and Fluids Sciences Section, Department of Applied Physics, Delft University of Technology, 2628 CJ Delft, The Netherlands
[2] Department of Physics, Pondicherry Central University, Pondicherry-605014, India

E-mail: nibu@ws.tn.tudelft.nl

Received 4 March 2002
Published 18 April 2002
Online at stacks.iop.org/JPhysCM/14/4509

Abstract

In this paper we report the thermal diffusivity of coconut shell measured using a laser-induced photoacoustic (PA) technique. An open PA cell in the heat transmission configuration is employed for the investigation. Laser-induced heating of the coconut shell is found to result in a thermoelastic bending of the sample. Taking into account this effect, an appropriate modification of Rosencwaig–Gersho theory for the PA effect is made for the calculation of the thermal diffusivity. Our investigation shows that coconut shell possesses a larger thermal diffusivity than ordinary wood.

1. Introduction

Coconuts grow on tropical palm trees scientifically known as *Cocos nucifera*. Coconut shell is similar to hard woods in chemical composition though the lignin content is higher and the cellulose content is lower. Since it has good durability characteristics, high toughness and abrasion-resistant properties, coconut shell is suitable for long-term use such as in utensils for household use and in handicrafts. Coconut shell powder is preferred over the alternative materials available in the market such as bark powder, furfural and peanut shell powder because of its uniformity in quality and chemical composition, better properties in respect of water absorption and resistance to fungal attack. Coconut shell powder manufactured from matured coconut shells finds extensive use in plywood and laminated board industry as a phenolic extruder. It is also used successfully with specialized surface-finishing liquid products (as an absorbent), mastic adhesives, resin casting and bituminous products, is used in heavy-duty hand-cleaner pastes as a mild abrasive, can give a smooth and lustrous finish to moulded articles, and also improves their resistance to moisture and heat, and is used as a mild abrasive in shot blasting of delicate objects and of historic buildings. In Asia, coconut shell powder is

[3] Author to whom any correspondence should be addressed.

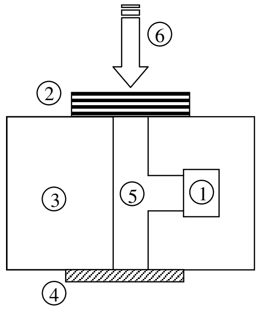

Figure 1. A cross-sectional view of the OPC. 1: microphone; 2: the multilayer sample; 3: the perspex body; 4: the glass window; 5: the gas chamber; 6: the incident laser beam.

widely used for the manufacture of insect repellent in the form of mosquito coils. Coconut shell-based activated carbon also finds a variety of applications in industry due to its several advantages over carbon made from other materials. It has high density, high purity and is virtually dust-free. Also, the pore structure is very uniform, with the majority of pores falling in the micro-pore range (5–10 Å) which is particularly effective for air and water purification applications.

In spite of the fact that coconut shell is so widely used in a variety of applications, its thermal properties have not yet been thoroughly investigated. In this paper we report the thermal diffusivity of a dried mature coconut shell. The thermal diffusivity is defined by $\alpha = k/\rho C$, where k is the thermal conductivity, ρ the density and C the specific heat capacity. The thermal diffusivity is a significant thermophysical parameter that determines the heat transport through a material. We used an open photoacoustic cell (OPC) in the heat transmission configuration for the investigation. The OPC configuration is of one of the latest photoacoustic (PA) detection schemes (George *et al* 2002, Perondi and Miranda 1987). OPCs are usually used for the investigation of thermal properties of solid samples. However, in some reports made in very recent years the uses of an OPC configuration for the study of liquid crystal and polymer samples are explained (George *et al* 2001a, 2001b).

2. Experimental procedure

In the OPC, usually, the solid sample is mounted directly on top of the microphone, leaving a small volume of air in between the sample and the microphone. Consequently, this configuration is a minimum-volume PA detection scheme and hence the signal strength is much greater than that from a conventional PA configuration. A cross-sectional view of the OPC used for the measurements is shown in figure 1. This homemade OPC is fabricated on an acrylic (perspex) disc of thickness 1 cm and diameter 5.5 cm (George and Vinayakrishnan 2001). The acoustic chamber is made by drilling a bore of diameter 3 mm, along the thickness direction, at the centre of the disc. One end of this cylindrical hole is closed with an optical quality glass slide of thickness 1.4 mm and the other end is left open. Another fine bore of diameter 1.5 mm pierced at the middle of the main chamber and directed perpendicular to it serves as the acoustic coupler between the main chamber and the microphone. At a distance of 8 mm from the main chamber the microphone is firmly glued to the orifice of the side tube. Shielded wires are used to take the electrical connections directly from the microphone. The entire system is then fixed inside a cylindrical hollow block of aluminium.

The experimental set-up used for the present investigation is given elsewhere (George *et al* 1999). The rear-side illumination or the so-called heat transmission configuration is adopted for the measurements. The coconut shell is fixed to the top of the air chamber of

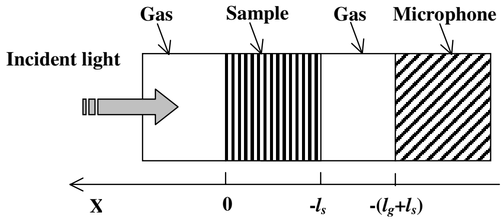

Figure 2. A schematic representation of the OPC geometry.

the OPC using vacuum grease and the sample is irradiated at its surface facing the ambient. Continuous-wave laser emission at 488 nm from an argon-ion laser (Liconix 5000) is used as the excitation beam. The laser beam has a $1/e^2$ diameter of 1.2 mm and is used without further focusing to minimize the lateral heat flow. Laser power of 70 ± 0.35 mW is employed for the measurements. A mechanical chopper (Stanford Research Systems SR530) is used to modulate the pump beam at the desired frequency. The PA signal is produced in a small volume of air in between the sample and the microphone. The signal is detected using a highly sensitive electret microphone (Knowles BT 1834) kept in the side chamber. Output of the microphone, for different modulation frequencies is processed using a dual-channel digital lock-in amplifier (Stanford Research Systems SR830).

3. Methodology and results

The Rosencwaig–Gersho (RG) theory for the PA effect is essentially a one-dimensional heat flow model, which explains the PA signal generation in a homogeneous sample (Rosencwaig and Gersho 1976). According to RG theory, with gas–microphone detection of the PA signal, the signal depends on the acoustic pressure disturbance at the sample–gas interface. The generation of the surface pressure disturbance, in turn, depends on the periodic temperature at the sample–gas interface. Exact expressions for this temperature are derived in the RG model, but the transport of the acoustic disturbance in the gas is treated in an approximate heuristic manner. Consider the OPC geometry shown in figure 2. If the sample is optically opaque, then all of the energy will be absorbed at the sample surface itself. When a sinusoidally modulated light beam of intensity I_0 is incident on a solid sample with an absorption coefficient β, the heat density generated at any point x due to the light absorbed at this point can be represented by

$$\tfrac{1}{2}\beta I_0 e^{\beta x}(1 + \cos\omega t). \tag{1}$$

For an experimental configuration as shown in figure 1, according to RG theory, we can prove that the periodic pressure variation in the air chamber in between the sample and the detector is given by

$$Q_{th} = \frac{\gamma P_0 I_0 (\alpha_g \alpha_s)^{1/2}}{2\pi T_0 l_g k_s f} \frac{e^{j(\omega t - \pi/2)}}{\sinh(l_s \sigma_s)} \tag{2}$$

where the nomenclature is as follows: γ is the ratio of the specific heat capacities of air, P_0 and T_0 are the ambient pressure and temperature, f is the modulation frequency. l_i, k_i and α_i are the thickness, thermal conductivity and the thermal diffusivity of the medium i, where $i = g$ refers to the gas and $i = s$ refers to the solid sample. Also $\sigma_i = (1 + i)a_i$, where $a_i = (\pi f/\alpha)^{1/2}$ is the thermal diffusion coefficient of the medium i. In arriving at the above expression it is assumed that the heat flux into the air in contact with the irradiated surface of the sample is negligible.

For a thermally thin sample (i.e., $l_s a_s \ll 1$), equation (2) reduces to

$$Q_{th} \cong \frac{\gamma P_0 I_0 \alpha_g^{1/2} \alpha_s}{(2\pi)^{3/2} T_0 l_g l_s k_s} \frac{\mathrm{e}^{\mathrm{i}(\omega t - 3\pi/4)}}{f^{3/2}}. \tag{3}$$

That is, the amplitude of the PA signal decreases as $f^{-1.5}$.

At high modulation frequencies, such that the sample is thermally thick (i.e., $l_s a_s \gg 1$),

$$Q_{th} \cong \frac{\gamma P_0 I_0 (\alpha_g \alpha_s)^{1/2}}{\pi T_0 l_g k_s} \frac{\mathrm{e}^{-l_s\sqrt{\pi f/\alpha_s}}}{f} \mathrm{e}^{\mathrm{i}(\omega t - \pi/2 - l_s a_s)}. \tag{4}$$

Equation (4) means that, for a thermally thick sample, the amplitude of the OPC signal decreases exponentially with the modulation frequency as $(1/f)\exp(-b\sqrt{f})$, where $b = l_s\sqrt{\pi/\alpha_s}$, whereas the phase decreases linearly with $\sqrt{f}$ with a slope of b. Hence, the thermal diffusivity α_s of the sample can be easily evaluated from either a signal amplitude plot or a phase plot. A necessary condition for employing the OPC configuration is that the sample should be optically opaque at the incident wavelength. Though the phase and amplitude of the PA signal contain clear signatures of the thermal transport properties of the sample, phase data are more reliable since the amplitude data depend on many external parameters such as sample surface quality and the detector response at different modulation frequencies.

However, in the case of plate-shaped solid samples, the contribution to the PA signal from the thermoelastic bending of the sample cannot be neglected, especially when the sample is in the thermally thick regime. A detailed analysis of this effect is discussed by Charpentier *et al* (1982) and Leite *et al* (1987). The thermoelastic bending is essentially due to the temperature gradient generated within the sample across its thickness. The existence of the temperature gradient causes an expansion of the sample parallel to its surface, thereby inducing bending of the sample along the thickness direction. Such a vibrating sample acts as a mechanical piston; this is otherwise known as the drum effect. In the thermally thick regime, the pressure fluctuation in the air chamber of the OPC detector resulting from the thermoelastic displacement, for an optically opaque sample, is given by

$$Q_{el} \cong \frac{3\alpha_T R^4 \gamma P_0 I_0 \alpha_s}{4\pi R_c^2 l_s^2 l_g k_s f} \left[\left(1 - \frac{1}{z}\right)^2 + \frac{1}{z^2}\right]^{1/2} \mathrm{e}^{\mathrm{i}(\omega t + \pi/2 + \phi)} \tag{5}$$

where $z = b\sqrt{f}$, $\phi = \tan^{-1}(1/(z-1))$ and α_T is the sample thermal-expansion coefficient. R is the radius of the front hole of the microphone and R_c is the radius of the OPC air chamber. Equation (5) means that the thermoelastic contribution, at high modulation frequencies (such that $z \gg 1$), varies as f^{-1}, and its phase ϕ follows the expression

$$\phi_{el} \cong \phi_0 + \tan^{-1}(1/(z-1)). \tag{6}$$

Thus, for a thermally thick sample, if the thermoelastic contribution is dominant, the thermal diffusivity can be evaluated from the modulation-frequency dependence of the signal phase (equation (6)).

The coconut shell we use is obtained from a coconut grown in Kerala, India. The shell is dried in sunlight for several days and the fibres at the outer surface is carefully removed. Both sides of a 1 cm × 1 cm piece of the sample are then polished using fine emery paper to get a uniform thickness of 0.9 mm. The dark brown specimen is optically opaque at the excitation wavelength. The OPC signal phase variation obtained from this sample as a function of the laser modulation frequency is shown in figure 3. It is very clear from the plot that the experimental data do not show a linear response as predicted by RG theory (equation (4)). The solid curve in figure 3 corresponds to a theoretical fit of equation (6) to the experimental data. The close agreement of the theoretical plot and experimentally observed data is a clear indication of the

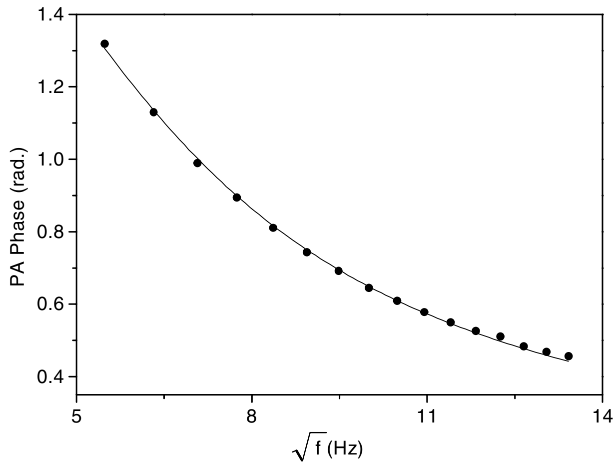

Figure 3. Variation of OPC signal phase as a function of modulation frequency. Here the black dots correspond to the experimental data points and the solid curve is the best theoretical fit of equation (6) to the experimental data.

thermoelastic bending of the sample due to laser-induced heating. The thermal diffusivity of the sample obtained from the fit to the experimental data is 0.4738 cm^2 s^{-1}. This value is much greater than the thermal diffusivity value of ordinary wood (*Wood Handbook* 1999).

Acknowledgments

The measurements were carried out at the optoelectronics laboratory of the International School of Photonics (ISP), Cochin University of Science and Technology, Cochin-682022, India. The authors are grateful to Professors V P N Nampoori, C P G Vallabhan and P Radhakrishnan of ISP.

References

Charpentier P, Lepoutre F and Bertrand L 1982 *J. Appl. Phys.* **53** 608
George N A, Kumar B A, Radhakrishnan P and Vallabhan C P G 1999 *J. Phys. D: Appl. Phys.* **32** 1745
George N A, Vallabhan C P G, Nampoori V P N, George A K and Radhakrishnan P 2001a *Appl. Phys.* B **73** 145
George N A, Vallabhan C P G, Nampoori V P N, George A K and Radhakrishnan P 2001b *J. Phys.: Condens. Matter* **13** 365
George N A and Vinayakrishnan R 2001 *Lasers Eng.* **11** 283
George N A, Vallabhan C P G, Nampoori V P N and Radhakrishnan P 2002 *Opt. Eng.* **41** 251
Leite N F, Cella N, Vargas H and Miranda L C M 1987 *J. Appl. Phys.* **61** 3025
Perondi L F and Miranda L C M 1987 *J. Appl. Phys.* **62** 2955
Rosencwaig A and Gersho A 1976 *J. Appl. Phys.* **47** 64
Wood Handbook—Wood as an Engineering Material 1999 (Madison, WI: Forest Products Laboratory, USDA Forest Service) ch 3